



# HHS Public Access

Author manuscript

*Nat Cell Biol.* Author manuscript; available in PMC 2012 October 01.

Published in final edited form as:

*Nat Cell Biol.* ; 14(4): 424–430. doi:10.1038/ncb2451.

## Homeostatic control of recombination is implemented progressively in mouse meiosis

Francesca Cole<sup>1</sup>, Liisa Kauppi<sup>2</sup>, Julian Lange<sup>2</sup>, Ignasi Roig<sup>2,\*</sup>, Raymond Wang<sup>1</sup>, Scott Keeney<sup>2,3</sup>, and Maria Jasin<sup>1</sup>

<sup>1</sup>Developmental Biology Program, Memorial Sloan-Kettering Cancer Center, 1275 York Ave, New York, NY 10065 USA

<sup>2</sup>Molecular Biology Program, Memorial Sloan-Kettering Cancer Center, 1275 York Ave, New York, NY 10065 USA

<sup>3</sup>Howard Hughes Medical Institute, Memorial Sloan-Kettering Cancer Center, 1275 York Ave, New York, NY 10065 USA

### Abstract

Humans suffer from high rates of fetal aneuploidy, often arising from the absence of meiotic crossover recombination between homologous chromosomes<sup>1</sup>. Meiotic recombination is initiated by double-strand breaks (DSBs) generated by the SPO11 transesterase<sup>2</sup>. In yeast and worms, at least one buffering mechanism, crossover homeostasis, maintains crossover numbers despite variation in DSB numbers<sup>3–8</sup>. We show here that mammals display progressive homeostatic control of recombination. In wild-type mouse spermatocytes, focus numbers for early recombination proteins (RAD51, DMC1) were highly variable from cell to cell, whereas foci of the crossover marker MLH1 showed little variability. Furthermore, mice with greater or fewer copies of the *Spo11* gene — with correspondingly greater or fewer numbers of early recombination foci — displayed relatively invariant crossover numbers. Homeostatic control is enforced during at least two stages, after the formation of early recombination intermediates and later while these intermediates mature toward crossovers. Thus, variability within the mammalian meiotic program is robustly managed by homeostatic mechanisms to control crossover formation, probably to suppress aneuploidy. Meiotic recombination exemplifies how order can be progressively implemented in a self-organizing system despite natural cell-to-cell disparities in the underlying biochemical processes.

---

Meiotic DSBs initiate a complex cell biological program in which their repair is coupled to chromosome pairing and synapsis, leading to the formation of crossovers. Crossovers

---

Users may view, print, copy, download and text and data- mine the content in such documents, for the purposes of academic research, subject always to the full Conditions of use: [http://www.nature.com/authors/editorial\\_policies/license.html#terms](http://www.nature.com/authors/editorial_policies/license.html#terms)

Correspondence and requests for materials should be addressed to S.K. (s-keeney@ski.mskcc.org) and M.J. (m-jasin@ski.mskcc.org).

\*Cytology and Histology Unit, Department of Cell Biology, Physiology, and Immunology, Universitat Autònoma de Barcelona, Barcelona, Spain

Author contribution F.C., L.K., J.L., I.R., R.W. performed experiments. F.C., S.K., and M.J. wrote the paper.

### Competing financial interests

The authors declare no competing financial interests.

physically link homologous chromosomes to ensure accurate segregation at the first meiotic division. DSBs are processed to generate single-stranded DNA onto which the RAD51 and DMC1 proteins load to mediate strand invasion of the homologous chromosome. Pairing and synapsis of homologs ensues while recombination intermediates mature through several steps and DSB repair is completed. Although the control mechanisms are not well understood, each homolog must have at least one crossover (the obligate crossover) and crossovers do not form close to one another (interference)<sup>9</sup>. Recently, in budding yeast and nematodes, crossover homeostasis has been described in which crossover numbers are maintained even with variation in DSB numbers<sup>3, 5–8</sup>. This safeguarding of crossovers comes at the expense of noncrossovers<sup>5</sup>, an alternative recombination outcome. However, it is unclear what the targets of this homeostatic control are or when during recombination this control is imposed. In mice as few as 10% of meiotic DSBs are repaired as crossovers and many homologs experience only a single crossover, indicating that progression from DSB formation to maturation of the final crossover product is highly regulated.

To determine whether homeostatic control of meiotic recombination exists in mammals, and if so, when it occurs, we characterized recombination intermediates cytologically in wild-type mouse spermatocytes. RAD51 and DMC1 mark early intermediates, whereas MSH4 localizes to a subset of later, transitional ones, a fraction of which are subsequently marked by MLH1 at mid-pachynema<sup>10, 11</sup> (Fig. 1a). These MLH1 foci label ~90% of mammalian crossover sites. Consistent with earlier reports, we observed that numbers of RAD51 and DMC1 foci peak at early zygonema, whereas fewer MSH4 and then MLH1 foci are observed at later prophase stages (Fig. 1b). The decline in recombination focus numbers as meiosis progresses likely reflects sites that have been or will be resolved as noncrossovers, as well as rare sites that will be resolved by MLH1-independent crossover pathways<sup>12</sup>.

Cell-to-cell differences in numbers of recombination foci were dynamic, with early foci more variable than later ones. To quantify this pattern, we determined the ratio of the standard deviation to the mean, i.e., the coefficient of variation (CV; Fig. 1c). RAD51 and DMC1 foci had large CVs with overlapping 95% confidence intervals, implying substantial differences between spermatocytes in numbers of recombination intermediates. By contrast, the CV was significantly smaller for MSH4 foci and lower still for MLH1, with non-overlapping 95% confidence intervals. Thus, crossover numbers, as measured by MLH1 foci, are relatively constant despite highly variable early recombination intermediates, suggesting that recombination is homeostatically controlled in mice.

Homeostatic control would imply a cellular response to DSB perturbation<sup>5</sup>. To test this, we altered the number of active *Spo11* loci. Wild-type mice (*Spo11*<sup>wt</sup>) were compared to mice heterozygous for a *Spo11* null allele (*Spo11*<sup>het</sup>)<sup>13</sup> or overexpressing *Spo11* from a transgene (*Spo11*<sup>wt+tg</sup>), which encodes the SPO11β isoform<sup>14</sup>. SPO11 protein levels corresponded to the genetic locus number: compared with wild-type littermates, *Spo11*<sup>het</sup> mice expressed roughly half as much of the two major SPO11 isoforms (α and β), whereas *Spo11*<sup>wt+tg</sup> had approximately twice as much SPO11β (Fig. 2a).

Importantly, the mean number of RAD51 and DMC1 foci also trended with *Spo11* copy number in early meiotic prophase. Compared to *Spo11*<sup>wt</sup> mice, *Spo11*<sup>het</sup> mice had ~15%

fewer RAD51 foci and ~30% fewer DMC1 foci, whereas *Spo11<sup>wt+tg</sup>* mice had ~25% more RAD51 and DMC1 foci (Fig. 2b and Table 1). Differences between the *Spo11* genotypes were statistically significant, and all had similarly large CVs. The first, semi-synchronous wave of meiosis in juveniles yielded results comparable to those in adults (Fig. S1 and Table 1). It is notable, however, that the difference in foci between *Spo11<sup>wt</sup>* versus *Spo11<sup>het</sup>* or *Spo11<sup>wt+tg</sup>* mice was less than the expected two-fold difference predicted from SPO11 protein levels. We also quantified  $\gamma$ H2AX, the phosphorylated form of the histone variant H2AX that is made in response to SPO11-generated DSBs<sup>15</sup>. *Spo11<sup>het</sup>* mice showed on average about half the level of SPO11-dependent  $\gamma$ H2AX as *Spo11<sup>wt</sup>* mice, and, conversely, *Spo11<sup>wt+tg</sup>* mice had on average about twice the level of  $\gamma$ H2AX as *Spo11<sup>wt</sup>* littermates (Figs 2c and S2). Thus, altered *Spo11* copy number resulted in a quantitative change in markers for early recombination intermediates.

Remarkably, mean MLH1 focus numbers were indistinguishable between all three genotypes and showed uniformly small CVs (Figs 2d and S1; Table 1). Moreover, there was no significant difference in the percent of bivalents lacking an MLH1 focus (data not shown). These results reinforce the conclusion that mouse spermatocytes homeostatically control crossover numbers.

The progressive decrease in the CV for recombination foci in wild-type mice (Fig. 1c) — from >30% (RAD51, DMC1) to ~21% (MSH4) to ~11% (MLH1) — suggested that homeostatic control is not limited to one step in the meiotic recombination pathway. Given that recombination intermediates along the crossover pathway equalize for the different *Spo11* genotypes, we asked if RAD51 and DMC1 focus counts even out as meiotic prophase progresses and DSBs are repaired. Indeed, we found that all three *Spo11* genotypes had similar mean DMC1 focus numbers by late zygonema (Fig. 3b; Table 1), indicating that at least some degree of recombination homeostasis is implemented by this stage.

As with DMC1, mean RAD51 focus numbers also equalized by late zygonema for *Spo11<sup>wt</sup>* and *Spo11<sup>het</sup>* spermatocytes (Fig. 3a; Table 1). However, *Spo11<sup>wt+tg</sup>* mice showed different kinetics of RAD51 foci, with numbers already maximal at leptonema rather than early zygonema and then decreasing but not to the same level as the other genotypes (Fig. 3a). This pattern may reflect precocious and prolonged SPO11 $\beta$  transgenic expression, and hence DSB formation<sup>14</sup>. Consistent with precocious DSB formation, DMC1 focus numbers were also disproportionately high at leptonema in *Spo11<sup>wt+tg</sup>* mice, even though they eventually equalized with the other genotypes by late zygonema. Possibly, DSBs formed later in meiosis or persistent unrepaired DSBs resulting from transgene expression are shunted to a mitotic-like repair mechanism<sup>16</sup> and are less likely to engage the meiosis-specific DMC1.

The equilibration of DMC1 foci indicates that homeostatic control can be at least partially exerted by late zygonema, but does not address whether it is fully implemented by this stage. To test whether additional homeostatic control is imposed later, as suggested by results from wild-type mice, we examined MSH4 foci, which form coincident with DMC1 equilibration. Numbers of MSH4 foci correlated with SPO11 expression: *Spo11<sup>het</sup>* spermatocytes had 8.4% fewer MSH4 foci than wild type, and *Spo11<sup>wt+tg</sup>* spermatocytes had 7.0% more (Table 1;  $p < 0.0001$  and  $p = 0.002$ , respectively, one-tailed Mann-Whitney test). As these differences

between the genotypes were smaller than for early DMC1 or RAD51 foci, these results are consistent with at least partial implementation of homeostatic control by late zygonema when MSH4 foci are maximal. However, we conclude that a significant fraction of recombination intermediates are subject to a homeostatic mechanism later, during pachynema after homologs have fully synapsed: mean MSH4 focus numbers were still different between the *Spo11* genotypes at early pachynema (Fig. 3c), yet MLH1 foci were already equal upon first appearance at mid-pachynema. Thus, homeostatic control during meiotic recombination is enforced during at least two stages, after the formation of early recombination intermediates and later while these intermediates mature toward crossovers.

In the view of recombination as a self-organizing process, all manifestations of crossover control are mechanistically related<sup>3, 5, 9, 17</sup>. Homeostasis, interference, and obligatory crossover formation are all predicted if the basic logic involves a driving force for crossover designation accompanied by propagation of an inhibitory process along chromosomes which prevents additional crossovers from forming nearby<sup>5, 17, 18</sup>. In contrast, homeostasis and obligatory crossover formation do not follow from deterministic models in which DSBs are fated from the beginning to follow one of two (or more) non-overlapping pathways that generate either interfering or non-interfering crossovers<sup>19</sup>. Progressive implementation of homeostatic control is reminiscent of what is observed for interference, which has also been inferred to occur in at least two stages, at or before MSH4 focus formation and at or before MLH1 focus formation<sup>20</sup>. Hence, recombination homeostasis acts coincident with interference. A mechanistic relationship between these phenomena predicts that crossover interference would be similar in the three *Spo11* genotypes. We observed the same degree of interference irrespective of *Spo11* locus number (Fig. 4a and 4b). As MLH1 foci probably mark all interfering crossovers<sup>11</sup>, these results demonstrate that crossover interference is not affected by alterations in numbers of early recombination intermediates, consistent with homeostatic control of recombination and crossover interference arising from a single underlying mechanism<sup>18</sup>.

Mammals provide a counterpoint to the two organisms analyzed for crossover homeostasis. In yeast, chromosome pairing is dependent on recombination provoked by a large number of DSBs<sup>21</sup>, a large fraction of which (one-half or more) are resolved as crossovers<sup>22</sup>. Interference is relatively weak<sup>3, 5, 9</sup>. In contrast, worms make many fewer DSBs and these are dispensable for homologous pairing<sup>23</sup>. A smaller but still substantial fraction of DSBs generates crossovers, and both interference and homeostasis are near absolute in this organism<sup>4, 8</sup>. Mammals display yet a different combination: pairing requires recombination which is induced by a large number of DSBs<sup>13</sup> (as in yeast), but only a small fraction of DSBs become crossovers (fewer than in worms) and interference is strong but not absolute<sup>20</sup>. The widely different spectra of chromosome behavior make it difficult to simply extrapolate findings between organisms. In this context, that homeostasis and interference go hand in hand across phyla reinforces the conclusion that they are inextricably linked.

The decreasing variability in numbers of early, transitional, and late recombination foci in wild-type mice reported here provides clear evidence that mouse spermatocytes have homeostatic control of recombination, with the endpoint being exquisite crossover control (Fig. 4c). In principle this control could absorb differences of either absolute DSB number

or the kinetics of DSB formation and repair. *Spo11<sup>wt+tg</sup>* mice almost certainly experience increased absolute DSB numbers, as RAD51 and DMC1 foci at leptotema substantially surpass the counts in *Spo11<sup>het</sup>* mice at any stage. This result provides evidence for crossover homeostasis. That crossover homeostasis can compensate for increased DSB numbers also provides a new framework to understand prior studies of *Spo11<sup>+/-Atm<sup>-/-</sup></sup>* spermatocytes, which show only a modest (~10%) increase in MLH1 foci<sup>24</sup> despite an apparent ~6-fold increase in DSBs<sup>25</sup>. Constant MLH1 focus numbers in the face of increased absolute DSB levels implies that another recombination outcome absorbs the increase, presumably either interhomolog noncrossovers as in yeast<sup>3</sup>, recombination between sister chromatids<sup>26</sup>, non-interfering crossovers as in worms<sup>7, 27</sup>, or all three. RAD51 focus counts in *Spo11<sup>wt+tg</sup>* mice suggest the possibility of an additional layer of control with some breaks shunted to a mitotic-like recombination pathway, involving either the juxtaposed homolog or the sister chromatid<sup>16</sup>. In any case, our results suggest that homeostatic control of recombination pathway choice continues even after homologs are fully synapsed.

Removal of a single active copy of *Spo11* (*Spo11<sup>het</sup>*) may result in fewer DSBs, consistent with crossover homeostasis<sup>5</sup>. As interhomolog noncrossovers represent a substantial portion of DSB repair events in mouse spermatocytes<sup>28</sup>, they provide more than adequate “buffering” capacity to achieve crossover homeostasis. However, the large ratio of noncrossovers to crossovers limits the ability to discern the small changes in noncrossover numbers expected by altering *Spo11* locus number (Table S1). However, an alternative to reduced levels of DSBs is that *Spo11<sup>het</sup>* mice have modified kinetics of DSB formation and repair. Recent evidence implicates the ATM kinase in regulating SPO11 DSB formation in mouse spermatocytes through a negative feedback loop<sup>25</sup>. In *Spo11<sup>het</sup>* spermatocytes, reduced DSB formation early might yield less ATM kinase activation and thereby less inhibition of SPO11 DSB activity, ultimately resulting in equivalent DSB numbers as wild type, but with slower kinetics. In support of this interpretation, the concentration of γH2AX, a direct target of the ATM kinase, closely tracked with the number of active *Spo11* loci, while numbers of early recombination foci — DSB markers that are further downstream — were less directly proportional to *Spo11* copy number. If correct, this kinetic scenario would describe a different type of homeostasis, namely, control of DSB formation, which might work in conjunction with crossover homeostasis to provide robust, multi-layered control of meiotic recombination.

Recombination initiation by DSB formation is a stochastic process in that each meiotic cell’s DSB “map” is unique, with the location of crossovers (and noncrossovers) differing widely between individuals (e.g., <sup>3, 29</sup>). As a result, the breadth of sites engaged in recombination within a population works toward maximizing genetic diversity. We show here that another consequence of this stochasticity is highly variable numbers of DSBs, even among normal mammalian meiocytes. A possible negative outcome is that some cells receive significantly fewer DSBs than the population average, potentially causing chromosome missegregation because of failed crossover formation. Homeostatic control, as uncovered here, ensures that crossing over is robust in the face of capricious recombination initiation, enforcing order in the meiotic program despite cell-to-cell variation in the underlying biochemical process.

Consistent with this concept, mouse oocytes are similar to spermatocytes in displaying small CVs for MLH1 focus counts<sup>30, 31</sup> and comparably low aneuploidy rates<sup>32</sup>. Human spermatocytes probably have homeostatic mechanisms: from published data (for example, ref. <sup>33</sup>) we find that MLH1 focus counts in human spermatocytes have small CVs, in the same ~10% range as we observed for mouse. In marked contrast, MLH1 foci in human oocytes have a CV of >30%<sup>34</sup>, in the range observed for early recombination markers in mouse. Oocytes also missegregate chromosomes much more often than spermatocytes in humans<sup>1</sup>, raising the question of whether weaker homeostatic mechanisms in human oocytes are a root cause of the high fetal aneuploidy rates experienced by our species.

## METHODS

### Mice

All mice used in this study were of the C57BL6/J, 129X1/SvJ, or mixed C57BL6/J - 129X1/SvJ (Jackson Laboratories) backgrounds. The *Spo11* null allele has been described previously<sup>13</sup> and was genotyped by PCR, as previously described<sup>24</sup>. The *Spo11*<sup>wt+tg</sup> (wt+tg) mice are homozygous wild type at the endogenous *Spo11* locus and carry two allelic copies of a previously described *Spo11*@<sub>B</sub> transgene<sup>14</sup>. The transgene is expressed by a germ cell-specific promoter and was genotyped by Southern blotting<sup>14</sup>. All experimental animals were compared to wild-type littermates, with the exception of two *Spo11*<sup>wt+tg</sup> animals used for focus counts, which were compared instead to age-matched wild-type (not littermate) animals that were processed in parallel. Numbers of animals analyzed for each condition are listed in the figure legends and no significant inter-individual variation was noted. All experiments were performed in accordance with relevant regulatory standards and were approved by the MSKCC Institutional Animal Care and Use Committee.

### Spermatocyte chromosome spreads and immunofluorescence

Spermatocytes from adult (> 8 weeks old) or juvenile (11 to 13 dpp) mice were either surface spread<sup>24</sup> or separated into individual cells in suspension<sup>36</sup> prior to surface spreading. Immunofluorescence was performed as previously described<sup>24</sup>. Antibodies and dilutions used were SYCP3 (Abcam ab15093 at 1:500 and Santa Cruz sc-74569 at 1:500); RAD51 (EMD PC130 at 1:250); DMC1 (Santa Cruz sc-22768 at 1:200)<sup>37, 38</sup>; MSH4 (Abcam ab58666 at 1:200); MLH1 (BD Biosciences 51-1327GR at 1:75). After immunostaining slides were mounted in Prolong® Gold antifade reagent with DAPI (Invitrogen). Nuclei were staged by assessing the staining of SYCP3 with these criteria: leptoneuma, short stretches of axis with no evidence of thickening associated with synapsis; early zygonema, longer cohesive stretches of axis and some synapsis; late zygonema, greater than 50% synapsed axes, but not complete; early pachynema, completely synapsed axes, but less intensely stained sex body chromatin. The genotypes of the samples were blinded until after focus counts were determined. Only axis-associated foci were counted. MLH1 inter-focus distances were assessed as previously described<sup>38</sup>.

### Immunoprecipitation and western blotting

SPO11 immunoprecipitation and western blots were performed with adult littermates of the indicated genotypes as previously described for wt versus het<sup>39</sup> and for wt versus wt+tg<sup>14,25</sup>.

Protein levels between mice were confirmed to be equivalent by BioRad DC™ protein assay prior to immunoprecipitation. Quality and relative quantity of extracts were determined by Coomassie staining of whole cell extracts separated by SDS-PAGE. For  $\gamma$ H2AX experiments, decapsulated testes were homogenized by dounce and heated for 10 minutes at 95°C in RIPA buffer supplemented with protease (Roche) and phosphatase (Thermo Scientific) inhibitors. Extracts were then cleared by centrifugation. Protein levels in the whole cell lysate were quantified with the BioRad DC™ protein assay, equilibrated between littermates, and then boiled in 1x Laemmli buffer. Approximately 1/10 of juvenile testis samples was loaded per lane and fractionated by SDS-PAGE (15% gel). Gels were transferred to nylon membranes and western blotted with anti- $\gamma$ H2AX (Millipore, JBW301) by standard protocols. Equivalent loading was confirmed by quantification of a background band that cross-reacts with the anti- $\gamma$ H2AX antibody or by reprobing the blots (without stripping) with an antibody to  $\alpha$ tubulin (Sigma, T9026) (Fig. S3). Blots were developed with ECL™ reagent (GE Healthcare) and either directly captured with a Fujifilm Intelligent Dark Box LAS-3000 or exposed to film and scanned in a Kodak Image Station 4000R Pro. Bands of interest were quantified with ImageQuant.

### Statistical analysis

The Mann-Whitney test was applied to focus number comparisons to avoid assuming normal distribution. We used a one-tailed test as the expected alteration for reducing (*Spo11<sup>het</sup>*) or increasing (*Spo11<sup>wt+tg</sup>*) SPO11 activity is unidirectional. Confidence intervals of CVs were estimated by bootstrap resampling (10000 replicates, percentile method) using the “boot” package in R (version 2.13.1; <http://cran.r-project.org>).

Crossovers and noncrossovers at the A3 hotspot in *Spo11<sup>wt</sup>* and *Spo11<sup>het</sup>* mice were determined as previously described using C57BL/6/J  $\times$  DBA/2J F1 hybrid mice<sup>28</sup> (Table S1). Based on the ratio of crossovers to noncrossovers, a power analysis<sup>40</sup> was performed to determine the total number of recombinants required per genotype to ensure an 80% chance of observing a statistically significant result.

### Supplementary Material

Refer to Web version on PubMed Central for supplementary material.

### Acknowledgments

We thank current and past members of the Jasin and Keeney laboratories for helpful discussions. FC was supported by a Ruth L. Kirschstein NRSA (F32HD51392). S.K. is an Investigator of the Howard Hughes Medical Institute. This work was supported by NIH grant HD040916 (to M.J. and S.K.).

### References

1. Hassold T, Hall H, Hunt P. The origin of human aneuploidy: where we have been, where we are going. *Hum Mol Genet.* 2007; 16(Spec No. 2):R203–R208. [PubMed: 17911163]
2. Keeney, S. Spo11 and the formation of DNA double-strand breaks in meiosis. In: Egel, R.; Lankenau, D-H., editors. *Recombination and Meiosis*. Berlin Heidelberg: Springer-Verlag; 2007. p. 81-123.

3. Chen SY, et al. Global analysis of the meiotic crossover landscape. *Dev Cell*. 2008; 15:401–415. [PubMed: 18691940]
4. Hillers KJ, Villeneuve AM. Chromosome-wide control of meiotic crossing over in *C. elegans*. *Curr Biol*. 2003; 13:1641–1647. [PubMed: 13678597]
5. Martini E, Diaz RL, Hunter N, Keeney S. Crossover homeostasis in yeast meiosis. *Cell*. 2006; 126:285–295. [PubMed: 16873061]
6. Roig I, Keeney S. Probing meiotic recombination decisions. *Dev Cell*. 2008; 15:331–332. [PubMed: 18804427]
7. Youds JL, et al. RTEL-1 enforces meiotic crossover interference and homeostasis. *Science*. 2010; 327:1254–1258. [PubMed: 20203049]
8. Rosu S, Libuda DE, Villeneuve AM. Robust crossover assurance and regulated interhomolog access maintain meiotic crossover number. *Science*. 2011; 334:1286–1289. [PubMed: 22144627]
9. Jones GH, Franklin FC. Meiotic crossing-over: obligation and interference. *Cell*. 2006; 126:246–248. [PubMed: 16873056]
10. Cohen PE, Pollack SE, Pollard JW. Genetic analysis of chromosome pairing, recombination, and cell cycle control during first meiotic prophase in mammals. *Endocr Rev*. 2006; 27:398–426. [PubMed: 16543383]
11. Anderson LK, Reeves A, Webb LM, Ashley T. Distribution of crossing over on mouse synaptonemal complexes using immunofluorescent localization of MLH1 protein. *Genetics*. 1999; 151:1569–1579. [PubMed: 10101178]
12. Holloway JK, Booth J, Edlmann W, McGowan CH, Cohen PE. MUS81 generates a subset of MLH1-MLH3-independent crossovers in mammalian meiosis. *PLoS Genet*. 2008; 4:e1000186. [PubMed: 18787696]
13. Baudat F, Manova K, Yuen JP, Jasin M, Keeney S. Chromosome synapsis defects and sexually dimorphic meiotic progression in mice lacking Spo11. *Mol Cell*. 2000; 6:989–998. [PubMed: 11106739]
14. Kauppi L, et al. Distinct properties of the XY pseudoautosomal region crucial for male meiosis. *Science*. 2011; 331:916–920. [PubMed: 21330546]
15. Mahadevaiah SK, et al. Recombinational DNA double-strand breaks in mice precede synapsis. *Nat Genet*. 2001; 27:271–276. [PubMed: 11242108]
16. Larocque JR, Jasin M. Mechanisms of recombination between diverged sequences in wild-type and BLM-deficient mouse and human cells. *Mol Cell Biol*. 2010; 30:1887–1897. [PubMed: 20154148]
17. Zhang L, Kleckner NE, Storlazzi A, Kim KP. Meiotic double-strand breaks occur once per pair of (sister) chromatids and, via Mec1/ATR and Tel1/ATM, once per quartet of chromatids. *Proc Natl Acad Sci U S A*. 2011
18. Kleckner N, et al. A mechanical basis for chromosome function. *Proc Natl Acad Sci U S A*. 2004; 101:12592–12597. [PubMed: 15299144]
19. Stahl FW, Foss HM. A two-pathway analysis of meiotic crossing over and gene conversion in *Saccharomyces cerevisiae*. *Genetics*. 2010; 186:515–536. [PubMed: 20679514]
20. de Boer E, Stam P, Dietrich AJ, Pastink A, Heyting C. Two levels of interference in mouse meiotic recombination. *Proc Natl Acad Sci U S A*. 2006; 103:9607–9612. [PubMed: 16766662]
21. Cole F, Keeney S, Jasin M. Evolutionary conservation of meiotic DSB proteins: more than just Spo11. *Genes Dev*. 2010; 24:1201–1207. [PubMed: 20551169]
22. Mancera E, Bourgon R, Brozzi A, Huber W, Steinmetz LM. High-resolution mapping of meiotic crossovers and non-crossovers in yeast. *Nature*. 2008; 454:479–485. [PubMed: 18615017]
23. Dernburg AF, et al. Meiotic recombination in *C. elegans* initiates by a conserved mechanism and is dispensable for homologous chromosome synapsis. *Cell*. 1998; 94:387–398. [PubMed: 9708740]
24. Barchi M, et al. ATM promotes the obligate XY crossover and both crossover control and chromosome axis integrity on autosomes. *PLoS Genet*. 2008; 4:e1000076. [PubMed: 18497861]
25. Lange J, et al. ATM controls meiotic double-strand-break formation. *Nature*. 2011; 479:237–240. [PubMed: 22002603]
26. Goldfarb T, Lichten M. Frequent and efficient use of the sister chromatid for DNA double-strand break repair during budding yeast meiosis. *PLoS Biol*. 2010; 8:e1000520. [PubMed: 20976044]



27. Mets DG, Meyer BJ. Condensins regulate meiotic DNA break distribution, thus crossover frequency, by controlling chromosome structure. *Cell*. 2009; 139:73–86. [PubMed: 19781752]
28. Cole F, Keeney S, Jasin M. Comprehensive, fine-scale dissection of homologous recombination outcomes at a hot spot in mouse meiosis. *Mol Cell*. 2010; 39:700–710. [PubMed: 20832722]
29. Coop G, Wen X, Ober C, Pritchard JK, Przeworski M. High-resolution mapping of crossovers reveals extensive variation in fine-scale recombination patterns among humans. *Science*. 2008; 319:1395–1398. [PubMed: 18239090]
30. Baker SM, et al. Involvement of mouse Mlh1 in DNA mismatch repair and meiotic crossing over. *Nat Genet*. 1996; 13:336–342. [PubMed: 8673133]
31. de Boer E, Dietrich AJ, Hoog C, Stam P, Heyting C. Meiotic interference among MLH1 foci requires neither an intact axial element structure nor full synapsis. *J Cell Sci*. 2007; 120:731–736. [PubMed: 17298983]
32. Koehler KE, Schrumpp SE, Cherry JP, Hassold TJ, Hunt PA. Near-human aneuploidy levels in female mice with homeologous chromosomes. *Curr Biol*. 2006; 16:R579–R580. [PubMed: 16890511]
33. Ferguson KA, Leung S, Jiang D, Ma S. Distribution of MLH1 foci and inter-focal distances in spermatocytes of infertile men. *Hum Reprod*. 2009; 24:1313–1321. [PubMed: 19246465]
34. Lenzi ML, et al. Extreme heterogeneity in the molecular events leading to the establishment of chiasmata during meiosis I in human oocytes. *Am J Hum Genet*. 2005; 76:112–127. [PubMed: 15558497]
35. Bellani MA, Boateng KA, McLeod D, Camerini-Otero RD. The expression profile of the major mouse SPO11 isoforms indicates that SPO11beta introduces double strand breaks and suggests that SPO11alpha has an additional role in prophase in both spermatocytes and oocytes. *Mol Cell Biol*. 2010; 30:4391–4403. [PubMed: 20647542]
36. Heyting C, Dietrich AJ. Meiotic chromosome preparation and protein labeling. *Methods Cell Biol*. 1991; 35:177–202. [PubMed: 1779856]
37. Dray E, et al. Molecular basis for enhancement of the meiotic DMC1 recombinase by RAD51 associated protein 1 (RAD51AP1). *Proc Natl Acad Sci U S A*. 2011; 108:3560–3565. [PubMed: 21307306]
38. Roig I, et al. Mouse TRIP13/PCH2 is required for recombination and normal higher-order chromosome structure during meiosis. *PLoS Genet*. 2010; 6
39. Neale MJ, Pan J, Keeney S. Endonucleolytic processing of covalent protein-linked DNA double-strand breaks. *Nature*. 2005; 436:1053–1057. [PubMed: 16107854]
40. Cohen, J. *Statistical power analysis for the behavioral sciences*. Edn. 2nd. Hillsdale N.J.: Lawrence Erlbaum Associates, Inc.; 1988.

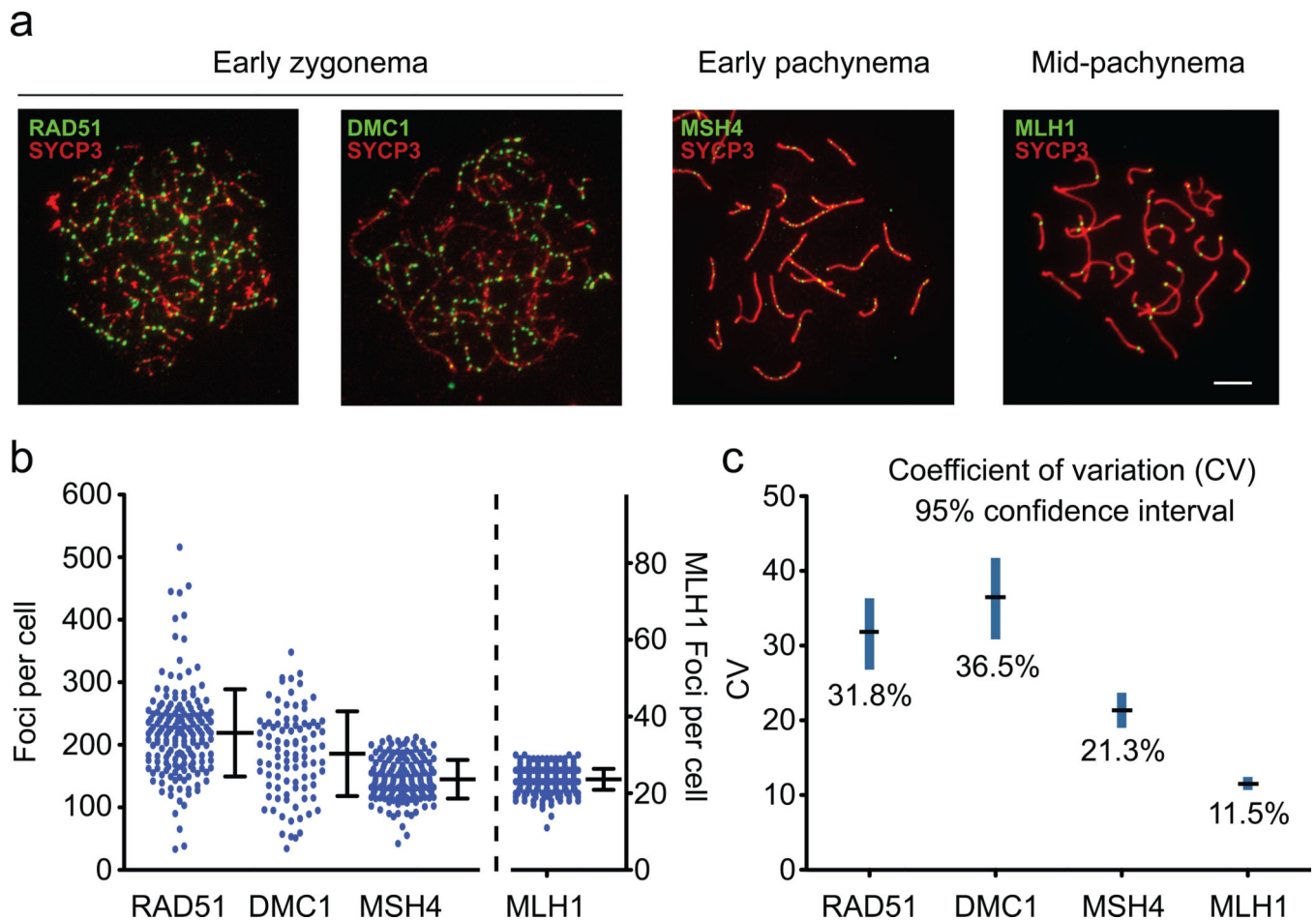


**Figure 1. Cell-to-cell variability in numbers of recombination intermediates decreases as meiotic prophase progresses**

**a)** Representative spermatocyte chromosome spreads from various meiosis prophase I stages, stained for the indicated proteins. Scale bar, 5  $\mu$ m.

**b)** Total foci per nucleus in wild-type spermatocytes. Each dot is the count from a single nucleus. Bars, mean  $\pm$  standard deviation (SD). RAD51 and DMC1 at early zygonema ( $219.2 \pm 69.8$  and  $185.8 \pm 67.8$ , respectively; mean  $\pm$  SD) and MSH4 at late zygonema and early pachynema ( $144.9 \pm 30.9$ ) are plotted on the left axis; MLH1 at mid-pachynema ( $23.6 \pm 2.7$ ) is plotted on the right axis (presented with the mean focus count at the same height as for MSH4, to facilitate comparison). Total mice analyzed: RAD51, n = 8; DMC1, n = 5; MSH4, n = 4; MLH1, n = 9.

**c)** Coefficients of variation (CV, black line) with 95% confidence intervals (blue line) estimated by bootstrapping (see Methods).

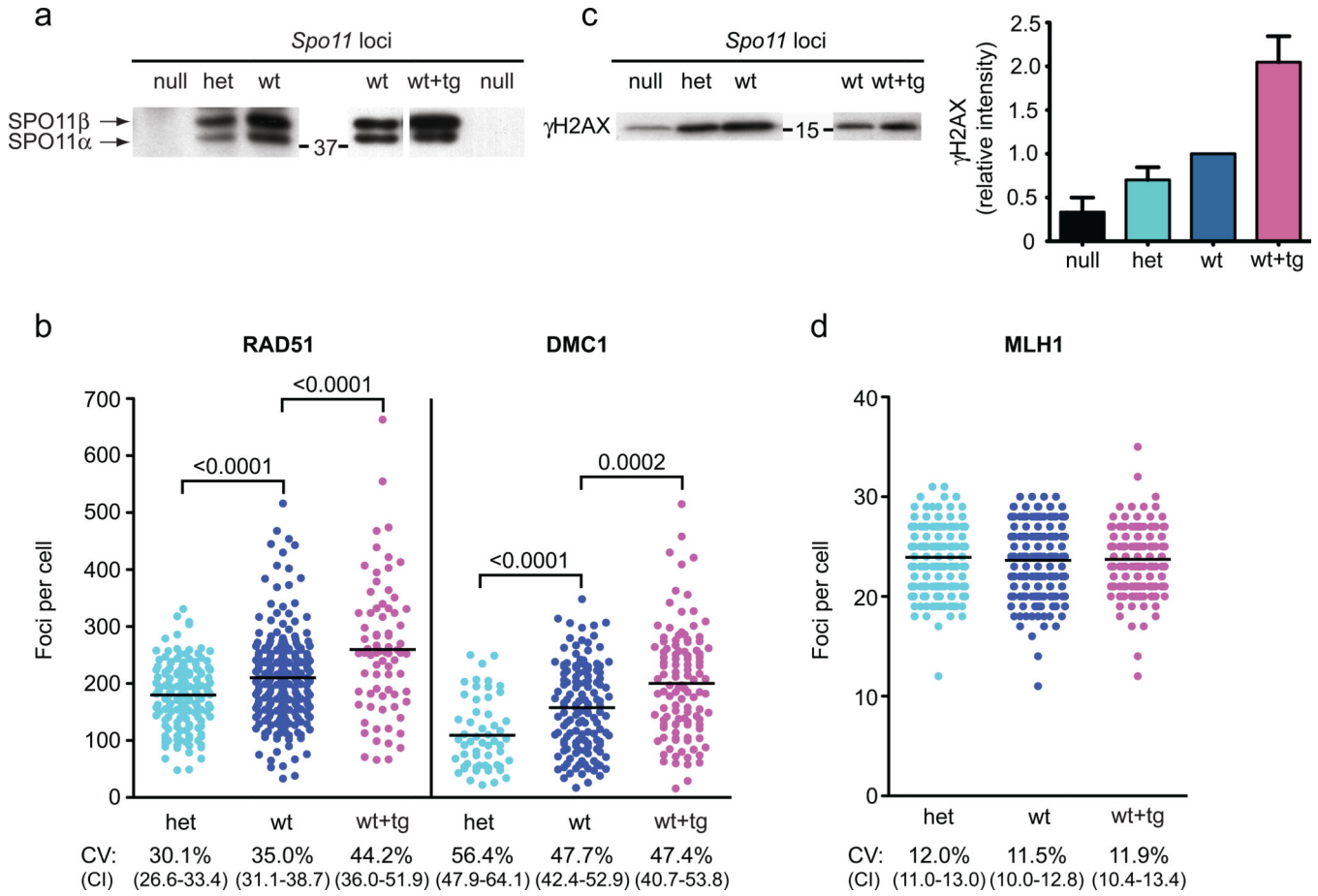


**Figure 2. *Spo11* locus number modulates early recombination indicators but not crossover numbers**

*Spo11<sup>het</sup>* and *Spo11<sup>wt+tg</sup>* mice are fertile and show no obvious meiotic defects, including no difference in the fraction of cells at various stages of meiotic prophase (data not shown).

**a** Immunoprecipitation followed by western blotting for SPO11 protein. *Spo11* locus composition: *Spo11<sup>null</sup>* (null), *Spo11<sup>het</sup>* (het), *Spo11<sup>wt</sup>* (wt), or *Spo11<sup>wt+tg</sup>* (wt+tg). The two major isoforms of SPO11 (α and β) are indicated on the left of the western blots, and the position of a molecular weight marker (kDa) is indicated in the center. Coomassie-stained gels were used to verify equivalent amounts of whole cell extracts from wt and het for immunoprecipitation (see Fig. S3a). The transgene expresses only SPO11β (which is known to be proficient for autosomal DSB formation<sup>14</sup>) such that SPO11α serves as standard for comparison. Representative blots from multiple experiments (n = 4) are shown.

**b** RAD51 and DMC1 foci in early meiotic prophase (leptonema and early zygonema, total early in Table 1) per nucleus in spermatocytes with the indicated genotypes. Each circle represents the focus count of a single nucleus. Black bars, means; brackets, p values for the indicated comparisons (Mann-Whitney, one-tailed). Mice analyzed: RAD51: het, n = 5; wt, n = 8; wt+tg, n = 3; DMC1: het, n = 2; wt, n = 5; wt+tg, n = 3.

**c** Left, whole cell extracts from juvenile testes 12 days post partum (dpp) immunoblotted for γH2AX protein. *Spo11* locus composition and the positions of molecular weight markers (kDa) as in (a). Right, quantification of γH2AX intensity relative to wild type in juvenile

testis extracts (mean  $\pm$  SD). Subtracting SPO11-independent  $\gamma$ H2AX determined from null mice, hets have on average 55% the level of  $\gamma$ H2AX (range ~30–70%) as wt, while wt+tg have twice the level (~180–240%). Number of independent mice analyzed and ages: null and het vs. wt, n = 5 (11 to 14 dpp); wt vs. wt+tg, n = 3 (12 dpp). Because SPO11-independent  $\gamma$ H2AX accompanies formation of the sex body later in meiosis<sup>15</sup>, we analyzed juvenile males whose testes contain leptotene and zygotene spermatocytes of the first semi-synchronous meiotic wave.

**d)** Autosomal MLH1 focus counts in mid-pachytene spermatocytes. Black bars show the means, which were not statistically significantly different (Mann-Whitney, one-tailed; het vs. wt,  $p > 0.07$ ; wt vs. wt+tg,  $p > 0.3$ ) Total mice analyzed: het, n = 7; wt, n = 9; wt+tg, n = 3. CV, coefficient of variation; CI, 95% confidence interval for the CV.

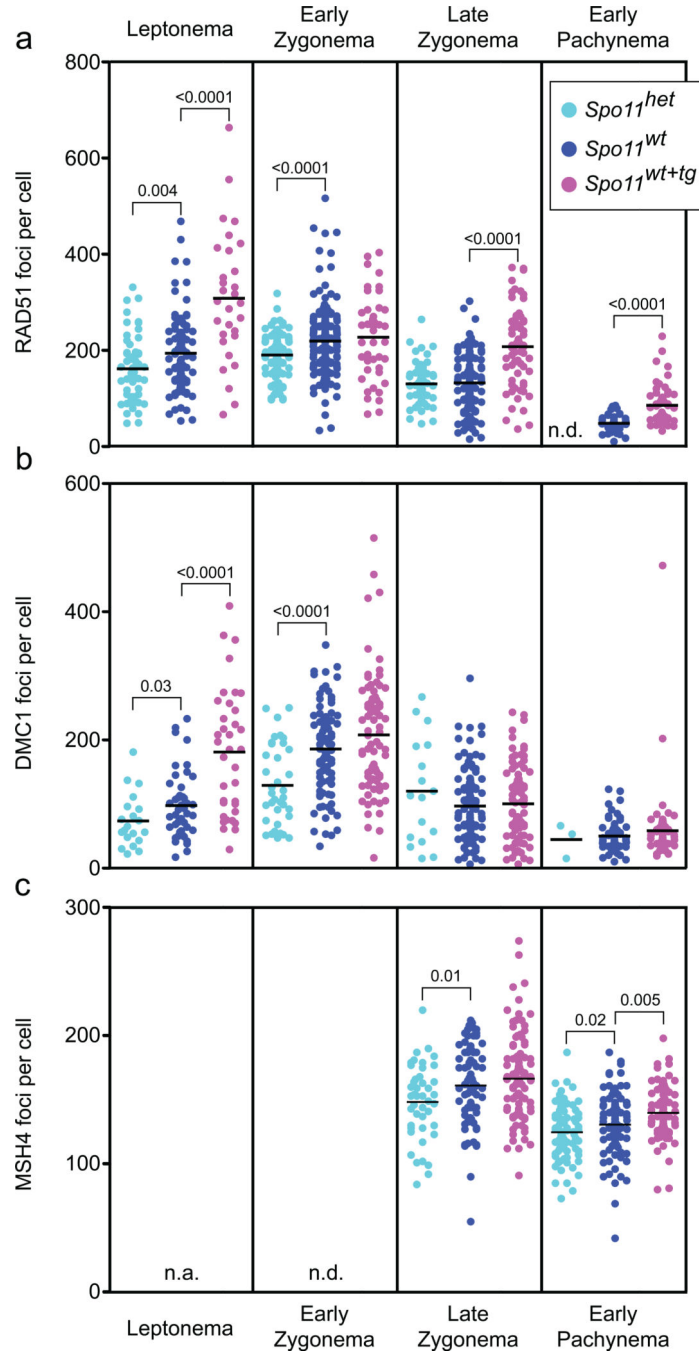


**Figure 3. Changes in numbers of recombination-associated foci as meiosis progresses**  
**a)** RAD51 foci at the indicated stages. Black bars, means; brackets, statistically significant p values (Mann-Whitney, one-tailed). Mice analyzed: *Spo11<sup>het</sup>*, n = 5; *Spo11<sup>wt</sup>*, n = 8; *Spo11<sup>wt+tg</sup>*, n = 3.  
**b)** DMC1 foci. Mice analyzed: *Spo11<sup>het</sup>*, n = 2; *Spo11<sup>wt</sup>*, n = 5; *Spo11<sup>wt+tg</sup>*, n = 3.  
**c)** MSH4 foci. Mice analyzed: *Spo11<sup>het</sup>*, n = 3; *Spo11<sup>wt</sup>*, n = 5; *Spo11<sup>wt+tg</sup>*, n = 3.  
 n.d., not determined; n.a., not applicable.

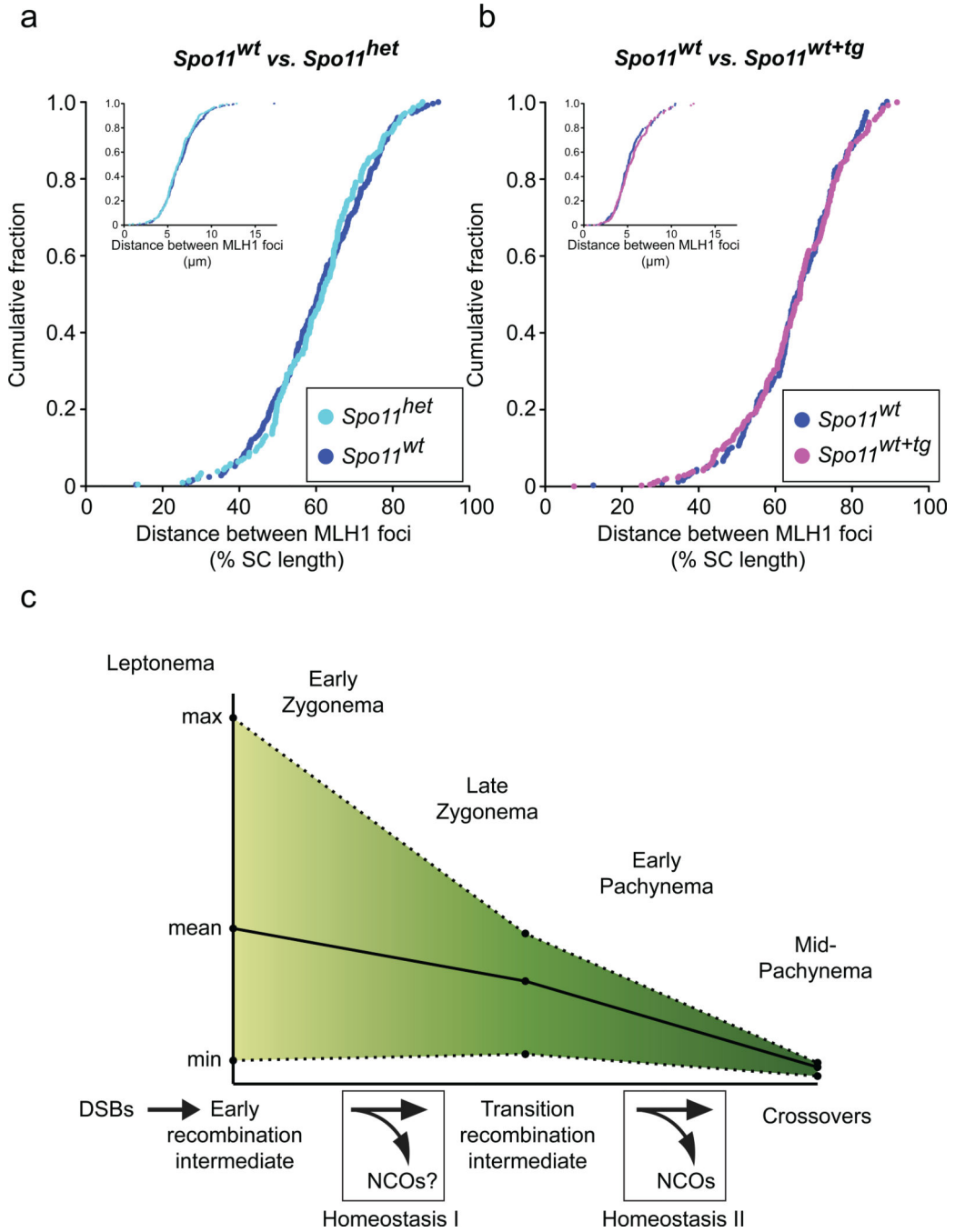


**Figure 4. Cytological interference is unchanged despite decreased or increased early recombination intermediates**

**a)** Cytological interference in *Spo11<sup>het</sup>* vs. *Spo11<sup>wt</sup>* spermatocytes. Distances between MLH1 foci were measured on autosomal bivalents containing two foci. The cumulative fraction of the inter-focus distances measured as a percentage of synaptonemal complex length or  $\mu\text{m}$  (inset) is shown. Number of bivalents analyzed: *Spo11<sup>het</sup>*,  $n = 206$ ; *Spo11<sup>wt</sup>*,  $n = 248$ . The *Spo11<sup>het</sup>* data was previously published<sup>24</sup>.

**b)** Cytological interference in *Spo11<sup>wt</sup>* vs. *Spo11<sup>wt+tg</sup>* spermatocytes. Number of bivalents analyzed: *Spo11<sup>wt</sup>*, n = 154; *Spo11<sup>wt+tg</sup>*, n = 192.

**c)** Homeostatic regulation of recombination occurs at two stages. Phases of meiotic prophase are indicated. Black line, wild-type mean focus counts for RAD51 (early recombination intermediate), MSH4 (transition recombination intermediate) and MLH1 (crossovers); dotted line, the maximal (max) and minimal (min) focus count for each marker. A model for progressive homeostatic implementation is depicted below. NCO, noncrossovers.

**Table 1**

Recombination focus frequencies in different mouse genotypes at different meiotic stages.

Marker	Stage	Genotype					
		<i>Spo11<sup>het</sup></i>		<i>Spo11<sup>wt</sup></i>		<i>Spo11<sup>wt+tg</sup></i>	
		Mean	CV	Mean	CV	Mean	CV
RAD51	Leptonema	161.6 <sup>a</sup>	39.8	194.0	40.0	308.2 <sup>a</sup>	43.8
	Early zygonema	190.3 <sup>a</sup>	23.3	219.2	31.8	227.2	38.0
	Late zygonema	130.3	33.0	132.0	44.6	207.6 <sup>a</sup>	38.7
	Early pachynema	n.d.	n.d.	48.2	36.4	85.5 <sup>a</sup>	48.2
	Total early <sup>c</sup>	179.9 <sup>a</sup>	30.1	210.1	35.0	259.6 <sup>a</sup>	44.2
DMC1	Juvenile	149.9 <sup>a</sup>	37.5	183.8	35.1	n.d.	
	Leptonema	73.6 <sup>a</sup>	56.2	97.6	53.2	181.2 <sup>a</sup>	54.1
	Early zygonema	129.1 <sup>a</sup>	48.4	185.8	36.5	208.0	44.7
	Late zygonema	120.2	68.4	96.75	55.9	100.4	59.2
	Early pachynema	44.7	59.3	50.1	46.3	58.3	103.6
MSH4	Total early <sup>c</sup>	109.3 <sup>a</sup>	56.4	157.7	47.7	200.3 <sup>a</sup>	47.4
	Late zygonema	148.4 <sup>a</sup>	19.7	161.2	19.0	166.6	19.4
	Early pachynema	124.8 <sup>a</sup>	16.2	130.7	17.9	139.9 <sup>a</sup>	14.6
MLH1 <sup>b</sup>	Total	132.7 <sup>a</sup>	19.6	144.9	21.3	155.1 <sup>a</sup>	19.8
	Mid-pachynema	23.9	12.0	23.6	11.5	23.7	11.9
	Juvenile	23.2	12.8	23.6	11.5	n.d.	

Means and coefficient of variation (CV) for each stage, genotype and marker tested. Two to nine independent mice were used for each marker (see figure legends). A similar decrease in RAD51 focus numbers was reported in mice heterozygous for a different *Spo11* knockout allele<sup>35</sup>.

<sup>a</sup> significantly different from wild type (p 0.05, Mann-Whitney, one-tailed).

<sup>b</sup> autosome foci only.

<sup>c</sup> Total early combines all focus counts for leptonema and early zygonema nuclei.

n.d., not determined.